Structure and strength of biocompatible coatings for titanium nickelide obtained in different reaction atmospheres

K. M. Dubovikov, *Post-Graduate Student, Research Engineer*[1], *e-mail: kirill_dubovikov@mail.ru*
A. S. Garin, *Post-Graduate Student, Research Engineer*[1]
A. A. Shishelova, *Student, Laboratory Assistant*[1]
M. A. Kovaleva, *Student, Laboratory Assistant*[1]

[1]*National Research Tomsk State University, Tomsk, Russia.*

The three layers Ti/Ni/Ti amorphous nanolaminate was applied to the TiNi substrate by magnetron sputtering. But subsequent synthesis provided in nitrogen and argon-nitrogen-carbonium dioxide atmospheres changed their phase composition and structure. The coating synthesized in nitrogen atmosphere consists mostly of the titanium nitrides but not from titanium oxides which were formed during synthesis in argon-nitrogen-carbonium dioxide atmosphere. Despite the fact that the nitrides have great hardness the scratch tests showed the coating synthesized in argon-nitrogen-carbonium dioxide atmosphere has better adhesion to the substrate. The load of 30 N is not enough for complete delamination of the coating. The results obtained with the aid of tensile tests demonstrated that the coating thickness less than 250 nm does not affect significantly on martensitic deformation of the TiNi phase.

Key words: titanium nickelide, magnetron sputtering, coating, SHS, adhesion, structure, tensile.
DOI: 10.17580/nfm.2022.02.08

Introduction

Titanium nickelide is quite a widespread material in medicine as it combines both bioactive and bioinert properties, including high corrosion resistance, good biochemical compatibility with body tissues, superelasticity and a shape memory effect [1–12]. The combination of all these properties makes titanium nickelide extremely popular in medicine.

Among the varieties of TiNi alloys, used in the manufacture of implants, it is especially worth noting the porous TiNi [7, 12]. The uniqueness of these porous materials is their wicking property, which is responsible for transporting liquids through interconnected pore channels. But the wettability, influencing the rate and height of lifting fluids in the capillaries, allows body tissues to penetrate into the internal structure of the material, which results in good adhesion of the living tissue to a porous TiNi implant [13].

Under the influence of aggressive chlorine-containing body fluids, TiNi alloys degrade, which is one of the main disadvantages of these alloys, since the material destruction leads to the leaching of nickel into the organic medium, surrounding this implant. Such leaching entails allergic reactions and tumor appearance [2, 7, 8]. Another task, which is no less important, is that of improving biocompatibility. Various corrosion-resistant biocompatible coatings are applied to the alloy to solve these two problems, using at the same time a variety of methods, beginning from the complex ones, for example, magnetron sputtering [14, 15], micro-arc oxidation [16, 17], and ending with conventional annealing in air [18]. When the bioactive properties of the surface are significantly improved by means of the coating, the bioinert properties frequently deteriorate, since the coating does not withstand high dynamic loads or has poor wear resistance, offered by the body [19, 20]. Its integrity is violated, cracks and chips appear, which also causes the yield of metal ions that may influence the body negatively. However, other coatings' biocompatibility or corrosion resistance is far from being the best [21, 22]. Considering all of the above-mentioned, creating a coating with good bioactive and bioinert properties in aggregate is really a very difficult and urgent task.

In this case, it is worth mentioning another important feature of porous TiNi alloys, i.e. those obtained by self-propagating high-temperature synthesis (SHS). This feature is a thin protective oxycarbonitride layer, formed during synthesis on the pore surfaces, which has an excellent corrosion resistance and does not interfere with the realization of the effects of superelasticity and shape memory [7]. The problem of this layer is the complexity of studying its structure and properties, since it is almost inaccessible, being on the pore surface. Therefore, the purpose of this work is to simulate the process of synthesizing the surface layers, occurring during SHS on a flat TiNi substrate by applying the Ti/Ni/Ti nanolaminate using magnetron sputtering, and to study the adhesion of the obtained coatings to the substrate, their strength and structure.

Materials and methods

The creation of the test samples consisted of two stages: applying the Ti/Ni/Ti nanolaminate to the TiNi substrate and synthesizing the resulting coatings in nitrogen and argon-nitrogen-carbon dioxide atmospheres.

The Ti/Ni/Ti nanolaminate layers with a total thickness of 150 nm were sprayed sequentially in a high-purity argon atmosphere in the system of magnetron sputtering onto polycrystalline TiNi plates. The substrate chemical composition included Ti = 49.72 ± 0.18, Ni = 50.28 ± ± 0.23 (at.%). The substrate with a polished surface was cleaned using an Ar^+ argon plasma ion source with a current of 70 mA and an accelerating voltage of 3.5 kV for 10 min. The magnetrons were located directly above the sample at an angle of 45° to each other. The layers were sprayed under the following conditions. The argon operating pressure was 1 Pa, the deposition time for Ti was 75 s and 30 s for Ni, the discharge voltage for Ti was 350 V and 420 V for Ni. The magnetron current for Ti was 2 A and 1 A for Ni, the substrate temperature was equal to room temperature, the argon consumption ϕ_{Ar} was 35 cm^3/min, the floating potential was (≈25 V) for substrate biasing. The distance from the substrate to the targets was 100 mm. In these conditions, the operating deposition rates were determined: 40 nm/min for titanium and 100 nm/min for nickel.

The subsequent synthesis was conducted in the SHS mode in two atmospheres: in nitrogen and in argon-nitrogen-carbon dioxide. The optimal temperature regimes of the synthesis were experimentally selected to initiate the reaction synthesis. SHS was initiated using point contact heating with direct current electrodes.

The phase composition, crystallinity of the samples with synthesized coatings, and the near-surface layers of the matrix were studied using *X*-ray diffraction on a Shimadzu XRD-6000 diffractometer in the Cu *K*α radiation in the standard mode in the symmetric Bragg-Brentano geometry of imaging (XRD) and in the grazing beam mode in the asymmetric geometry of imaging (GIXRD). The quantitative content of the phases, present in the coating, was estimated by means of the full-profile analysis by the Rietveld method using the POWDER CELL 2.4 software and the PDF4+ crystalline structure databases.

To analyze the samples by means of the transmission electron microscopy with a resolution of up to 0.14 nm, the TiNi samples were prepared by ion thinning. The Ti/Ni/Ti layers were sprayed sequentially. The Ti(*x*)Ni(*y*)(N,C) coatings were synthesized in the cross-section geometry using the EM-09100IS Ion Slicer unit (JEOL, Japan) for ion cutting and polishing.

The electron microscope investigations of thin foils were conducted by means of a transmission electron microscope JEM-2100 (Jeol, Japan) with an accelerating voltage of 200 kV in the modes of TEM (bright and dark fields) and diffraction contrast.

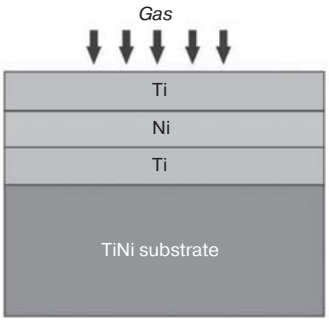

Fig. 1. Schematic representation of the amorphous nanolaminate synthesis in the gaseous atmosphere

The CSEM Micro Scratch Tester measuring unit and the "scratching" technique were used to determine the adhesive properties of the coatings. A scratch was applied on the surface of the system under study (coating-substrate) with a diamond indentor (of the Rockwell type with a working part radius of 20 μm) at a speed of 6.79 mm/min. During this process, a force (loading force) linearly increasing from 0.01 N to 30 N acted on the indentor. The rate of the load increase was 29.99 N/min.

Gradient coatings with a thickness of 150 nm and 5 μm were synthesized on the surface of the samples made from monolithic titanium nickelide of the TN-1 grade with dimensions of 0.2×0.2×50 mm. The samples with the coatings were subject to the uniaxial tensile test till their destruction using an INSTRON 3369 testing machine at a tensile speed of 1 mm/sec at room temperature according to GOST (State Standart) 1497–84.

Results

Fig. 2 shows the cross-section of the TiNi substrate with alternately applied Ti/Ni/Ti layers of a total thickness of 150 nm. The nanolaminate coating represents alternating amorphous layers with a corresponding diffuse halo shown in the diffraction patterns **(Fig. 2, *b*)**. The nanometer thickness of the sputtered layers will not hinder the superelastic behavior of the TiNi substrate.

As a result of synthesizing the Ti/Ni/Ti nanolaminate in the nitrogen atmosphere, a different coating structure has been formed **(Fig. 3)**. The outer layers (*I*, *II* and *III*) are represented by the gradient crystalline coating:

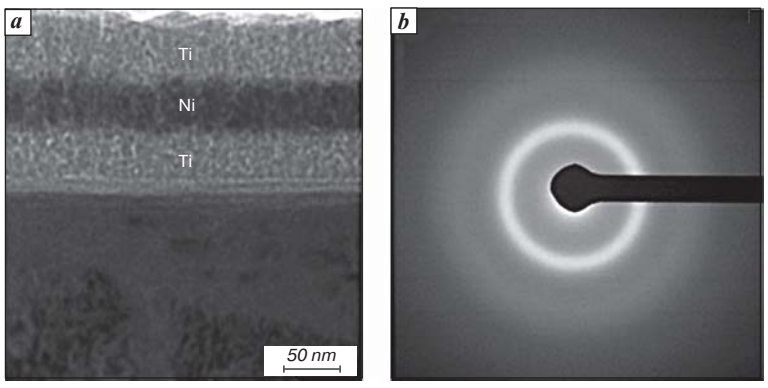

Fig. 2. Bright-field TEM-image of the nanolaminate before the synthesis (*a*) and the corresponding microdiffraction pattern (*b*)

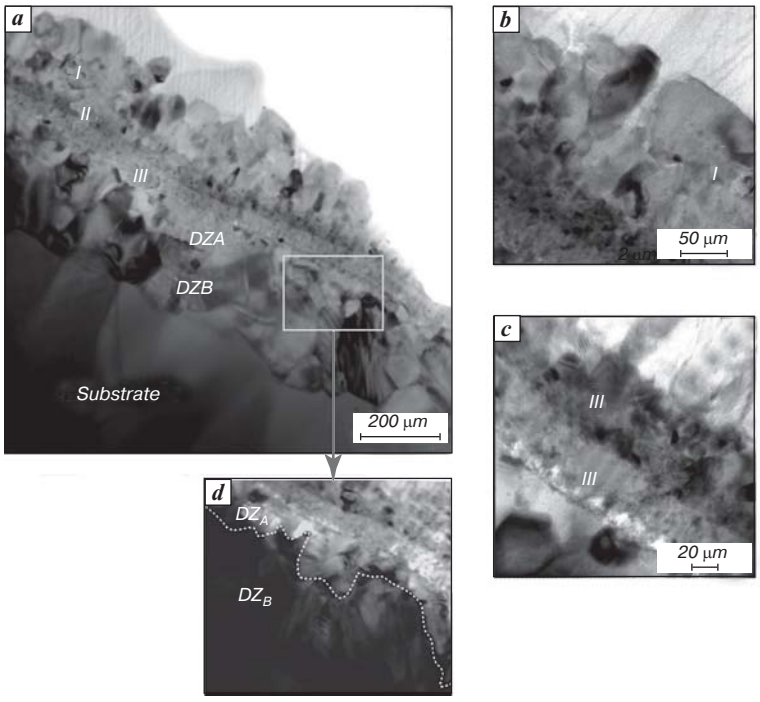

Fig. 3. General TEM-image of the coating, synthesized in nitrogen at 900 °C in the SHS mode (*a*); TEM-image of the first layer (*b*); TEM-image of the second and third layers (c); TEM-image of the diffusion zone (*d*)

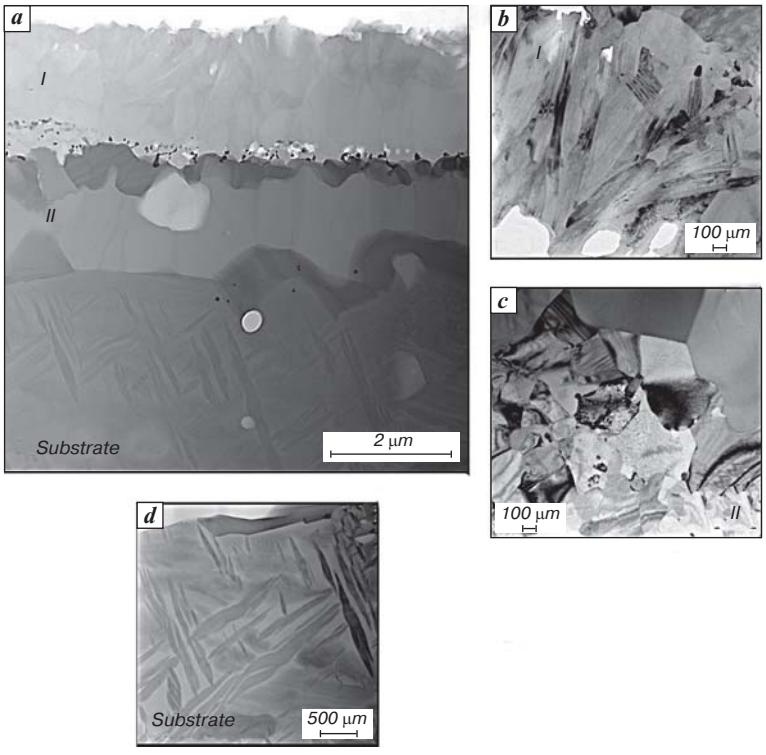

Fig. 4. General TEM-image of the coating, synthesized in argon-nitrogen-carbon dioxide at 900 °C in the SHS mode (*a*); TEM-image of the first layer (*b*); TEM-image of the second layer (diffusion zone) (*c*); TEM-image of the substrate (*d*)

I by TiO_2 + TiN; *II* by Ti_3Ni_4 + $Ti_4Ni_2(O,N)$; *III* by TiN **(Table 1)**. Region *I* has the most massive thickness of about 150 nm and an average size of disordered grains of about 40 ± 5 nm. Since the synthesis occurred in the nitrogen atmosphere, titanium formed largely just nitride compounds in outer layer *I*, whose 80% of the grains were oriented along [200]. Regions *II* and *III* with a thickness of 50 nm are already denser and consist of 8 ± 2-nanometer grains. Layer *II* is represented by Ti_3Ni_4 + $Ti_4Ni_2(N,O)$, where the $Ti_4Ni_2(N,O)$ solid solution has been formed as a result of nitrogen dissolution in Ti_2Ni, and the Ti_3Ni_4 phase has a limited ability to dissolve nitrogen (no more than 0.5 at.% at 900 °C). Layer *III*, consisting of TiN, results from SHS, which prevents the nitrogen diffusion from the atmosphere into the diffusion zone (DZA and DZB), represented by intermetallic phases $TiNi_3$ and $TiNiO_3$.

Since the second sample was synthesized in the mixed atmosphere, consisting of argon-nitrogen-carbon dioxide at 900 °C **(Fig. 4)**, interstitial impurities actively diffused into the amorphous Ti/Ni/Ti nanolaminate. As a result of this process, a solid two-layered crystalline structure was formed: the outer part was $Ti_2O_3(N,C)$ with a thickness of 2.5–3.0 μm and the inner layer was $TiNi_3$ + + $Ti_4Ni_2O(N,C)$ with a thickness of about 2.0 μm **(Table 1)**. The diffusion between the layers was nonuniform. The $Ti_2O_3(N,C)$ phase occupies approximately 50 % of the coating. A high degree of micro-distortions in the crystal lattice, as well as the deviation of the parameters from the reference ones, allows suggesting that nitrogen and carbon are present as interstitial impurities in the hexagonal structure. The diffusion zone consists of two

Table 1
Phase composition of the coating, diffusion zone, and substrate of the samples synthesized in three different atmospheres. The data are based on the XRD and GIXRD results

Coating synthesized in the nitrogen atmosphere	Coating	TiO_2 TiN Ti_3Ni_4 $Ti_4Ni_2(N,O)$
	Diffusion zone	$TiNiO_3$ $TiNi_3$
	Substrate	TiNi B2
Coating synthesized in the argon-nitrogen-carbon dioxide atmosphere	Coating	$Ti_2O_3(N,C)$
	Diffusion zone	$Ti_4Ni_2O(N,C)$ $TiNi_3$
	Substrate	TiNi B19′

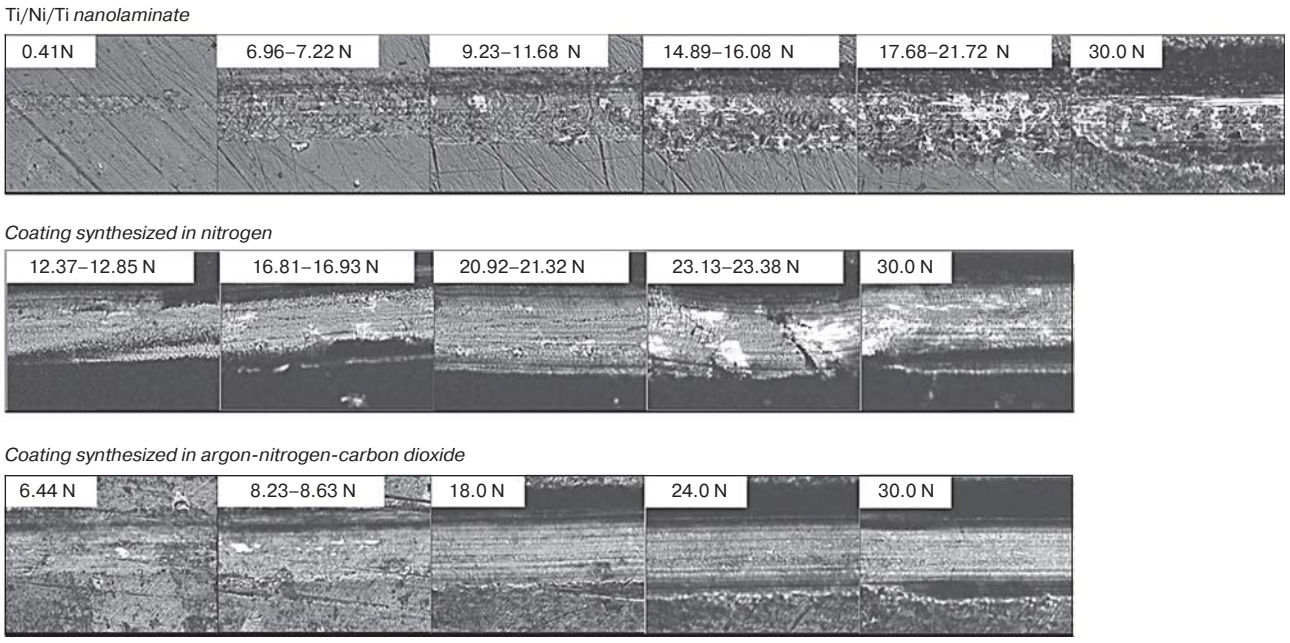

Fig. 5. Optical images of the surface of the coated samples during scratch tests

phases $Ti_4Ni_2O(N,C)$ and $TiNi_3$ that are approximately similar in volume fractions.

The scratch test was used to assess the strength of coating adhesion to the substrate **(Fig. 5)**. The initial amorphous nanolaminate, applied to the substrate, begins to disintegrate under the load equal to 7 N. Since the load increases linearly, the number of microcracks, chips and delaminations of the coating increases over time. In case of the amorphous Ti/Ni/Ti nanolaminate, a load of 15-16 N can be considered critical despite the fact that under 30 N there is no complete coating delamination.

Due to the synthesis in the nitrogen atmosphere, a coating, consisting of nitrides and titanium oxides, was formed. The coating slightly detached under a load of 13 N; the coating detached critically and microcracks formed under a load of 23 N. But at the same time, a load of 30 N is insufficient for complete detachment of the coating.

The coating, obtained in the argon-nitrogen-carbon dioxide atmosphere, demonstrates the origination of a defect when exposed to a load of 6.44 N; when increasing the load up to about 8 N, minor detachments of the coating appear, but it is worth noting that a further increase in the load entails no destruction. The analysis of the obtained results allowed concluding that the sample, synthesized in the argon-nitrogen-carbon dioxide atmosphere, has a better adhesive strength compared to that of the coating, obtained in the nitrogen atmosphere.

It was noted that the oxycarbonitride coating, formed naturally during SHS, did not influence in any way the physical and mechanical properties of the TiNi matrix, which has the shape memory effect and superelasticity. Therefore, to establish the permissible thickness of the coating, with which the mechanical properties would not deteriorate, an experiment on stretching the uncoated substrate and two samples with the coatings 250 nm and 5 μm thick, obtained in the argon-nitrogen-carbon dioxide atmosphere, was conducted **(Fig. 6)**. The results of the mechanical tests allowed establishing the fact that the tensile strength of the uncoated TiNi substrate was 1220 MPa. The application of the coatings 250 nm and 5 μm thick allowed increasing this value to 1320 and 1800 MPa, respectively **(Table 2)**. But the maximum sustained deformation decreased from 18.6 % for the uncoated TiNi to 16.5 and 12.6% for the samples with the coatings 250 nm and 5 μm thick, respectively. A coating of a greater thickness has a higher strength and a greater value of the martensite shear stress; besides, the yield-point area length is reduced from 10 to 7%. In view of this, the coatings with a thickness of

Table 2
Mechanical properties of the titanium nickelide alloy with the coating obtained in the argon-nitrogen-carbon dioxide atmosphere of different thicknesses

TiNi samples	σ_m, MPa	σ_B, MPa	E, GPa	ε_e, %	ε_m, %	ε_{pl}, %	ε_{tot}, %
Uncoated	780 ± 9	1220 ± 9	71 ± 1	1.1 ± 0.1	8.8 ± 0.3	8.6 ± 0.2	18.5 ± 0.3
With the 250-nm coating	810 ± 11	1320 ± 9	71 ± 1	1.1 ± 0.1	8.9 ± 0.3	6.5 ± 0.3	16.5 ± 0.2
With the 5-μm coating	1100 ± 18	1800 ± 11	99 ± 2	1.2 ± 0.1	5.8 ± 0.2	5.6 ± 0.4	12.6 ± 0.3

Notes: σ_m – martensite shear stress; σ_B – ultimate tensile strength; E – elastic modulus; ε_e – elastic deformation; ε_m – martensite deformation; ε_{pl} – plastic deformation; ε_{tot} – total strain-to-fracture.

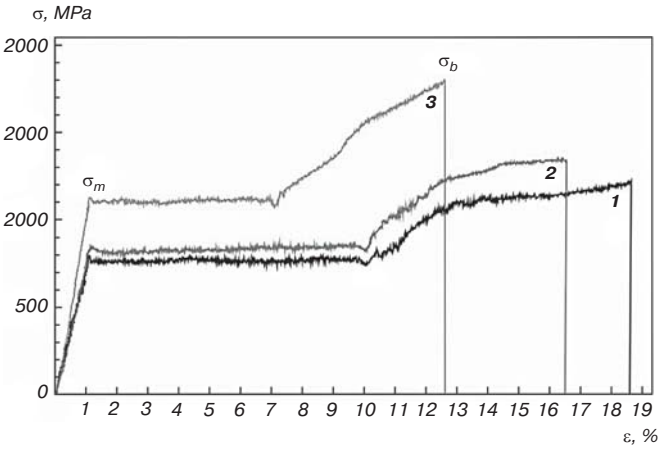

Fig. 6. Tensile stress-strain diagrams of monolithic titanium nickelide alloys:
1 – uncoated; *2* – with the coating, obtained in the argon-nitrogen-carbon dioxide atmosphere, 250 nm thick; *3* – with the coating, obtained in the argon-nitrogen-carbon dioxide atmosphere, *5* μm thick

less than 250 nm do not limit the inelastic super-tensile deformation of the titanium nickelide substrate, exerting a slight nonessential influence on the martensite deformation of the major TiNi phase during tensile tests.

Conclusion

The Ti/Ni/Ti nanolaminate with a thickness of 150 nm on the TiNi substrate was obtained by means of magnetron sputtering, and the subsequent synthesis was conducted in two different atmospheres: in nitrogen and in argon-nitrogen-carbon dioxide. The synthesis in each of the atmospheres was found to influence differently on the qualitative composition and morphology of the coating, but at the same time they all have a gradient structure. The kinetics and mechanisms of the phase formation when synthesized in different atmospheres were studied. The coatings with a thickness of less than 250 nm were found not to limit the inelastic super-tensile deformation of the titanium nickelide substrate, exerting a slight inessential influence on the martensite deformation of the major TiNi phase during tensile tests. The scratch tests showed that the coating, synthesized in the argon-nitrogen-carbon dioxide atmosphere, had the highest strength of adhesion to the substrate. Therefore, such coating can be potentially used to create articular implants.

Acknowledgment

The authors express their gratitude to the Doctor of Physical and Mathematical Sciences, Marchenko E. S., and the Candidate of Physical and Mathematical Sciences, Baigonakova G. A., NR TSU, for their assistance in writing the manuscript. "The research was conducted at the expense of the grant of the Russian Science Foundation, No. 19-72-10105, https://rscf.ru/project/19-72-10105/"

References

1. Kuchumov A. G., Lokhov V. A., Slovikov S. V., Wildemann V. E., Straube G. I., Sutorihin D. A. Experimental Investigation of Shape Memory Alloys Utilized in Medicine. *Russian Journal of Biomechanics*. 2009. Vol. 13, Iss. 3. pp. 7–19.

2. Wever D. J., Veldhuizen A. G., Sanders M. M., Schakenraad J. M., van Horn J. R. Cytotoxic, Allergic and Genotoxic Activity of a Nickel-Titanium Alloy. *Biomaterials*. 1997. Vol. 18, Iss. 16. pp. 1115–1120.

3. Kokorev O. V., Khodorenko V. N., Baigonakova G. A., Marchenko E. S., Yasenchuk Yu. F., Gunther V. E., Anikeev S. G., Barashkova G. A. Metal-Glass-Ceramic Phases on the Surface of Porous TiNi-Based SHS-Material for Carriers of Cells. *Russian Physics Journal*. 2019. Vol. 61, Iss. 9. pp. 1734–1740.

4. Witkowska J., Sowińska A., Czarnowska E., Płociński T., Rajchel B., Tarnowski M., Wierzchoń T. Structure and Properties of Composite Surface Layers Produced on NiTi Shape Memory Alloy by a Hybrid Method. *Journal of Materials Science: Materials in Medicine*. 2018. Vol. 29, Iss. 8. 110.

5. Olier P., Barcelo F., Béchade J., Brachet J., Lefevre E., Guenin G. Effects of Impurities Content (Oxygen, Carbon, Nitrogen) on Microstructure and Phase Transformation Temperatures of Near Equiatomic TiNi Shape Memory Alloys. *Journal de Physique IV (Proceedings)*. 1997. Vol. 7, Iss. C5. pp. 143–148.

6. Potekaev A. I., Klopotov A. A., Matyunin A. N., Marchenko E. S., Gyunter V. E., Dzhalolov Sh. A. The Influence of Phase Hardening on Premartensitic States and on Martensitic Transformation in Multicomponent Alloys Ti(Ni, Co, Mo) with Shape Memory Effects. *Inorganic Materials: Applied Research*. 2011. Vol. 2, Iss. 4. pp. 387–394.

7. Medical Materials and Implants with Shape Memory. In 14 vols. Vol. 1. Medical Materials with Shape Memory. Ed. by Gyunter V. E. Tomsk: NII meditsinskikh materialov i implantov s pamyatyu formy SFTI pri TGU, 2011. 533 p.

8. Mo nik P. A., Kosec T. Critical Appraisal of the Use and Properties of Nickel–Titanium Dental Alloys. *Materials*. 2021. Vol. 14, Iss. 24. 7859.

9. Ohtsu N., Yamasaki K., Taniho H., Konaka Y., Tate K. Pulsed Anodization of TiNi Alloy to Form a Biofunctional Ni-Free Oxide Layer for Corrosion Protection and Hydrophilicity. *Surface and Coatings Technology*. 2021. Vol. 412. 127039.

10. Gunther V., Radkevich A., Kang S., Chekalkin T., Marchenko E., Gyunter S., Pulikov A., Sinuk I., Kaunietis S., Podgorniy V., Chang M. J., Kang J. H. Study of the Knitted TiNi Mesh Graft in a Rabbit Cranioplasty Model. *Biomedical Physics & Engineering Express*. 2019. Vol. 5, Iss. 2. 027005.

11. Gyunter V., Marchenko E., Chekalkin T., Baigonakova G., Kim Ji-soon, Kang Ji-hoon, Klopotov A. Study of Structural Phase Transitions in Quinary TiNi(MoFeAg)-Based Alloys. *Materials Research Express*. 2017. Vol. 4, Iss. 10. 105702.

12. Chang H. I., Wang Y. Cell Responses to Surface and Architecture of Tissue Engineering Scaffolds. In: *Regenerative Medicine and Tissue Engineering – Cells and Biomaterials* (Ed. by D. Eberli). London: IntechOpen, 2011. pp. 569–588.

13. Ponsonnet L., Reybier K., Jaffrezic N., Comte V., Lagneau C., Lissac M., Martelet C. Relationship Between Surface

Properties (Roughness, Wettability) of Titanium and Titanium Alloys and Cell Behavior. *Materials Science and Engineering: C*. 2003. Vol. 23, Iss. 4. pp. 551–560.

14. Shanaghi A., Souri A., Saedi H., Chu P.K. Effects of the Tantalum Intermediate Layer on the Nanomechanical Properties and Biocompatibility of Nanostructured Tantalum/Tantalum Nitride Bilayer Coating Deposited By Magnetron Sputtering on the Nickel Titanium Alloy. *Applied Nanoscience*. 2021. Vol. 11, Iss. 6. pp. 1867–1880.

15. Motazedian F., Zhang J., Wu Z., Jiang D., Sarkar S., Martyniuk M., Yan C., Liu Y., Yang H. Achieving Ultra-Large Elastic Strains in Nb Thin Films on TiNi Phase-Transforming Substrate by the Principle of Lattice Strain Matching. *Materials & Design*. 2021. Vol. 197. 109257.

16. Wang X., Liu F., Song Y. Enhanced Corrosion Resistance and in vitro Bioactivity of NiTi Alloys Modified with Pydroxyapatite-Containing Al_2O_3 Coatings. *Surface and Coatings Technology*. 2018. Vol. 344. pp. 288–294.

17. Yeşildal R., Karabudak F., Şüküroğlu E. E., Şüküroğlu S., Zamanlou H., Bayındır F., Şen S., Totik Y. Differential Scanning Calorimetry (DSC) and Ni^{+2} Release Analysis of NiTi-Shape-Memory Dental Alloys Coated by Micro-Arc Oxidation (MAO) Method. *Applied Physics A*. 2018. Vol. 124. 572.

18. Mahmud A., Wu Z., Zhang J., Liu Y., Yang H. Surface Oxidation of TiNi and Its Effects on Thermal and Mechanical Properties. *Intermetallics*. 2018. Vol. 103. pp. 52–62.

19. Zhang K., Zhang H., Liu P., Zhang C., Li W., Chen X., Ma F. Electrophoretic Deposition of Graphene Oxide on NiTi Alloy for Corrosion Prevention. *Vacuum*. 2019. Vol. 161. pp. 276–282.

20. Horandghadim N., Khalil-Allaf J., Urgen M. Influence of Tantalum Pentoxide Secondary Phase on Surface Features and Mechanical Properties of Hydroxyapatite Coating on NiTi Alloy Produced by Electrophoretic Deposition. *Surface & Coatings Technology*. 2020. Vol. 386. 125458.

21. Rahimipour S., Salahinejad E., Sharifi E., Nosrati H., Tayebi L. Structure, Wettability, Corrosion and Biocompatibility of Nitinol Treated by Alkaline Hydrothermal and Hydrophobic Functionalization for Cardiovascular Applications. *Applied Surface Science*. 2020. Vol. 506. 144657.

22. Shanaghi A., Mehrjou B., Ahmadian Z., Souri A. R., Chu P. K. Enhanced Corrosion Resistance, Antibacterial Properties, and Biocompatibility by Hierarchical Hydroxyapatite/Ciprofloxacin-Calcium Phosphate Coating on Nitrided NiTi Alloy. *Materials Science & Engineering: C*. 2021. Vol. 118. 111524.

NFM